Lawrence Berkeley National Laboratory

Title
Electron dynamics and γ and e−e+ production by colliding laser pulses

Permalink
https://escholarship.org/uc/item/1wr6h35d

Authors
Jirka, M
Klimo, O
Bulanov, SV
et al.

Peer reviewed

Electron dynamics, γ and e^-e^+ production by colliding laser pulses

M. Jirka,[1,2] O. Klimo,[1,2] S. V. Bulanov,[3] T. Zh. Esirkepov,[3] E. Gelfer,[4] S. S. Bulanov,[5] S. Weber,[1] and G. Korn[1]

[1] *Institute of Physics of the CAS, ELI-Beamlines Project, Na Slovance 2, 182 21 Prague, Czech Republic*
[2] *Faculty of Nuclear Sciences and Physical Engineering,*
Czech Technical University in Prague, Brehova 7, 115 19 Prague 1, Czech Republic
[3] *Japan Atomic Energy Agency, Kansai Photon Science Institute,*
8-1-7 Umemidai, Kizugawa, Kyoto, 619-0215 Japan
[4] *National Research Nuclear University MEPhI, Kashirskoe shosse 31, Moscow, 115409 Russia*
[5] *Lawrence Berkeley National Laboratory, Berkeley, California 94720, USA*

The dynamics of an electron bunch irradiated by two focused colliding super-intense laser pulses and the resulting γ and e^-e^+ production are studied. Due to attractors of electron dynamics in a standing wave created by colliding pulses the photon emission and pair production, in general, are more efficient with linearly polarized pulses than with circularly polarized ones. The dependence of the key parameters on the laser intensity and wavelength allows to identify the conditions for the cascade development and γe^-e^+ plasma creation.

With the advent of 10 PW laser facilities, the new and so far unexplored field of ultra-intense laser matter interaction will become accessible experimentally [1]. The intensities of the order of 10^{23-24} W/cm² will be achieved in these interactions, therefore the possibility of efficient generation of gamma-ray photons or even electron-positron pairs has attracted much attention in the last decade (see review article [2] and references therein). In a strong electromagnetic field, electrons can be accelerated to such high energy that the radiation reaction starts to play an important role [3]. Moreover, a new regime of the interaction can be entered, dominated by quantum electrodynamics (QED) effects such as pair production and cascade development [2, 4]. If a photon with sufficient energy is emitted due to multiphoton Compton scattering and then interacts with n laser photons, new electron-positron pair can be created via the multiphoton Breit-Wheeler process [5]. Since the probabilities of the photon emission and pair creation depend on the particle momentum, on the electromagnetic field strength, and on their mutual orientation, it is necessary to elucidate the motion of electrons (positrons) in the electromagnetic field in the strong radiation reaction regime.

In this Letter we present the analysis of the electron motion and photon emission modeled as a discreet process in the electromagnetic (EM) standing wave (SW) generated by two colliding focused short super-intense laser pulses interacting with an electron bunch. The interaction of charged particles with an intense EM fields is characterized by two dimensionless relativistically invariant parameters [6]. First parameter is $a_0 = eE_0/m_e\omega_0 c$, the dimensionless EM field amplitude, which measures the energy gain of an electron over the field wavelength in units of $2\pi m_e c^2$. It is often referred to as the classical nonlinearity parameter. Here e and m_e are the electron charge and mass, E and ω_0 are EM field strength and frequency, c is the speed of light, respectively.

The second parameter is $\chi_e = [|(F_{\mu\nu}p_\nu)^2|]^{1/2}/m_e c E_S$ $(\chi_\gamma = [|(F_{\mu\nu}\hbar k_\nu)^2|]^{1/2}/m_e c E_S)$, where $E_S = m_e^2 c^3/e\hbar \simeq 1.3 \times 10^{18}$ V/m [7], $\hbar$ is the Planck constant, and $F_{\mu\nu}$ is the EM field tensor. The parameter $\chi_{e,\gamma}$ characterizes the interaction of electrons (positrons) and photons with the EM field. Depending on the energy of charged particles and field strength the interaction happens in one of the following regimes parametrized by a_0 and $\chi_{e,\gamma}$: (i) $a_0 > 1$, the electron dynamics is relativistic; (ii) $a_0 > \epsilon_{\text{rad}}^{-1/3}$, the interaction becomes radiation dominated; (iii) $a_0 > (2\alpha/3)^2\epsilon_{\text{rad}}^{-1}$ (or $\chi_e > 1$), the quantum effects begin to manifest themselves [8–10]; and (iv) $\chi_e > 1$, $\chi_\gamma > 1$, the interaction leads to an avalanche [11–14], the exponential growth of the electron-positrons and photons number. Here $\epsilon_{\text{rad}} = 4\pi r_e/3\lambda$ is the parameter indicating the strength of radiation reaction effects, $r_e = \alpha\hbar/m_e c$ is the classical electron radius.

We perform two-dimensional (2D) simulations of electron dynamics in a standing wave with the EPOCH code [15], based on Particle-in-Cell (PIC) method. Photon emission and e^-e^+ pair creation via the Breit-Wheeler process [5] are modeled using Monte-Carlo method. Two Gaussian laser pulses moving along the x-axis collide head-on in the center of the simulation box with the size of $40\lambda \times 40\lambda$. Each laser pulse has the wavelength of $\lambda = 1$ μm, period of $T = 2\pi/\omega$, focal spot full width at half maximum (FWHM) of $w_0 = 1.5\lambda$, FWHM duration of $9T = 30$ fs, intensity of 1.11×10^{24} W/cm² (so that $a_0 = 900$). We consider two cases of the laser polarization. The electric field oscillates along the y-axis in linearly polarized (LP) pulses and rotates about the x-axis in circularly polarized (CP) pulses. At the focal spot, $x = y = 0$, a 1λ diameter cloud of electrons is represented by 76,000 quasi-particles. Its density is $0.05n_c$, where $n_c = m_e\omega^2/4\pi e^2$ is critical density. In a moving reference frame the electron cloud can be considered as a bunch of electrons. The mesh size is $\lambda/100 = 10$ nm,

the time step is $\approx 0.01T$.

Colliding laser pulses create a transient EM SW. When they completely overlap, the electric field strength is zero at nodes, $x = (2n+1)\lambda/4$, and maximum at antinodes, $x = n\lambda/2$, where n is integer. The magnetic field nodes and antinodes are shifted by $\lambda/4$ with respect to the electric field. In an ideal infinite SW, the electric and magnetic fields remain zero in their respective nodes, while in their respective antinodes they synchronously oscillate along the polarization axis in the LP case or synchronously rotate about the x-axis in the CP case.

As seen in Fig. 1, the electron cloud is strongly distorted by colliding laser pulses. A part of electrons is expelled from the high-field region, mainly in the transverse direction. The observed asymmetry between up and down expelled electrons is due to the carrier-envelope phase difference of the laser pulses. Another part of electrons concentrates between the electric field antinodes. On each laser half-period, approximately one tenth of the electrons trapped near the electric field nodes are driven away in the transverse direction, Fig. 1 (near $x = \pm\lambda$, $y = -2\lambda$). In the case of CP, most electrons trapped in the SW are strongly localized near the electric field nodes $x = \pm\lambda/4$, Fig. 1(a). These electrons drift away from the focal spot in the transverse direction having relatively low value of χ_e parameter, $\chi_e < 0.05$. Higher χ_e parameter (≈ 0.5) is achieved by escaping electrons crossing few spatial periods of the SW.

In contrast to CP, in the case of LP electrons diffuse inside the SW period so that a significant number of electrons appear in the vicinity of the electric field antinodes, Fig. 1(b,c). These electrons typically acquire significantly higher χ_e parameter ($\gtrsim 1$) than in CP case. This leads to a more prolific emission of photons in the LP case. The electron concentration near antinodes has been emphasized in Ref. [16].

Figure 2 shows representative electron trajectories in the phase subspace (x, p_y, p_z) for CP (a,c) and (x, p_x, p_y) for LP (b,d), where x and p denote the electron longitudinal coordinate and momentum, respectively. Trajectories colored with respect to time in frames (a,b) show that some electrons quiver near electric field nodes or oscillate in the half of the SW spatial period, while others escape transiting through many spatial periods of the SW along the x-axis. In the CP SW, trapped electrons fall to the electric field nodes at $x = \pm\lambda/4$, Figs. 1(a), 2(a). The electron rotation at the electric field antinode is strongly unstable, so that particles quickly depart from antinodes to nodes. In the LP SW, electrons appear also at the nodes at $x = \pm3\lambda/4$, Figs. 1(b,c), 2(b).

Fig. 2(c,d) shows trajectories near the electric field node, colored according to the χ_e parameter. The electron momentum and χ_e are much greater in the LP case than in the CP case. These trajectories show dynamic features of strange attractors at electric field nodes and loops near antinodes predicted in Ref. [17] with a contin-
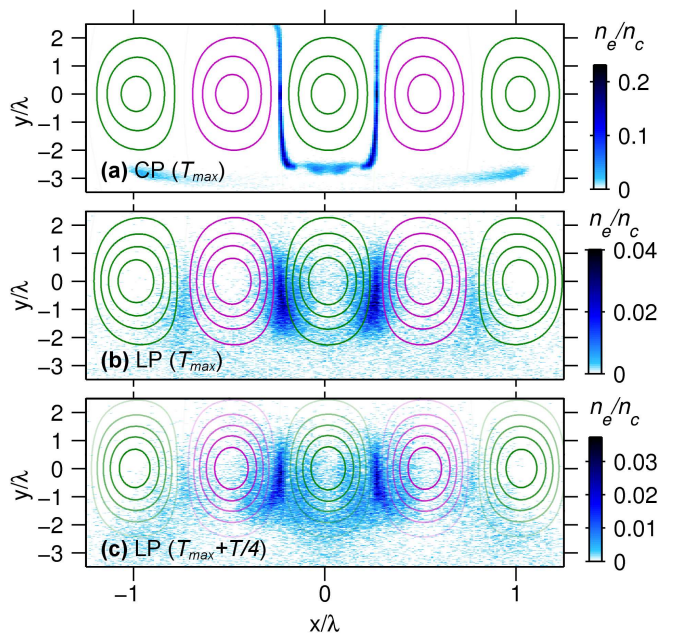

FIG. 1. Electron density (colorscale, n_e/n_c) in the (x, y) plane at $T_{\max}$, when the laser intensity is maximum in the focal spot, for different laser polarization: (a) CP, (b) LP, (c) LP at $T_{\max}+T/4$. Green (magenta) curves for positive (negative) electric field y-component.
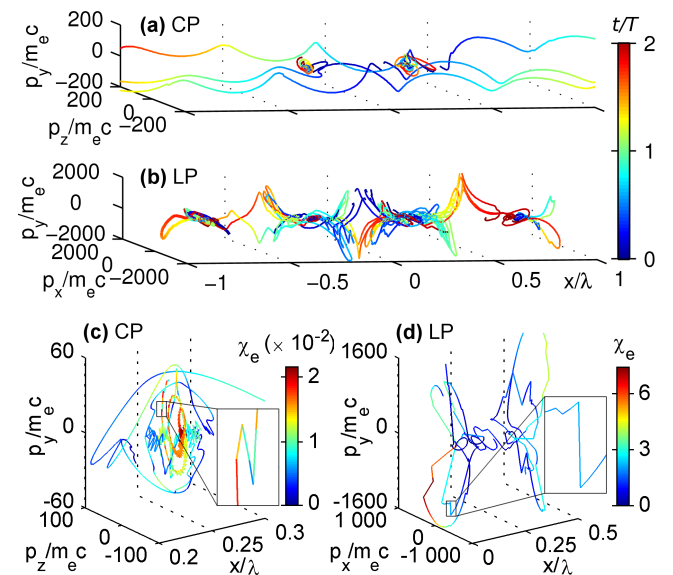

FIG. 2. Electron trajectories in the phase subspace for $T_{\max} < t < 2T_{\max}$ for (a,c) CP and (b,d) LP. Colorscale represents (a,b) time t in laser periods; (c,d) the electron χ_e parameter.

uous emission model. However, in this Letter the trajectories are not smooth, because of the quantum nature of the electron interaction with a high intensity EM field. The photon emission makes a sudden change of particle momentum. Since the probability of the multiphoton Compton effect corresponds to the emission of low energy
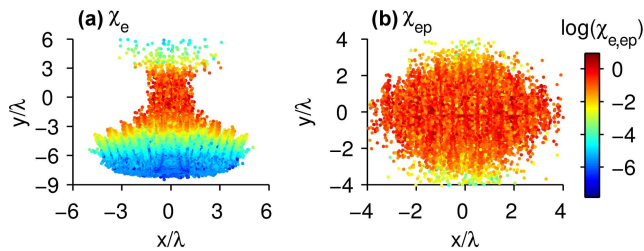
FIG. 3. Parameters χ_e and χ_{ep} for seed (a) and Breit-Wheeler (b) electrons, respectively, in the (x, y) plane at $T_{\max}$ for LP.
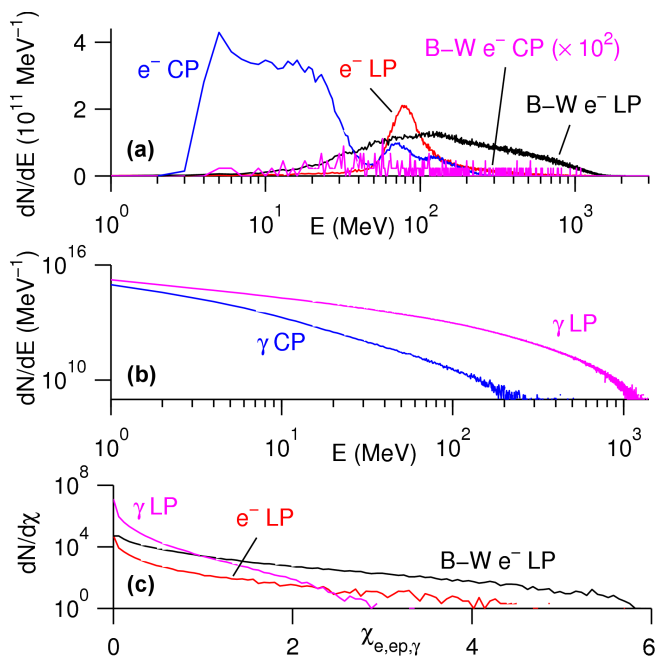

FIG. 4. Energy spectra of seed and Breit-Wheeler electrons (a), and photons (b) at $T_{\max}$ for different laser polarization. (c) Electron and photon distribution with respect to χ_e, χ_{ep} and χ_γ parameters for LP.

photons in most cases, the electron momentum change is relatively small. Being near an attractor, electrons after emission jump to another trajectory approaching the same or another attractor in the SW. Therefore, the attractors characteristic to CP and LP SW (such as strange attractors and loops) found with a continuous emission model reveal itself in the case when the discrete quantum nature of emission dominates the dynamics. In general, due to strongly dissipative dynamics, electrons "forget" their initial momentum and phase, therefore our conclusions concerning attractors remain valid also for high energy electron bunches, [17].

An emitted photon ballistically propagating through the SW creates an electron-positron pair via the Breit-Wheeler process. Since the photons emitted via the multistage Compton process have a power-law spectrum, the number of Breit-Wheeler pairs is mainly determined by the number of photons whose radiation length is about

the characteristic spatial extent of the EM SW [18]. When these Breit-Wheeler pairs are born in the volume occupied by intense EM field, they emit photons, thus increasing the photon number. Moreover, χ_{ep} parameter of newly created particles is higher than χ_e parameter of seed electrons for both CP and LP cases, Fig. 3. This is because Breit-Wheeler pairs are created near the EM field maxima.

Fig. 4(a,b) shows the energy spectra of seed electrons, Breit-Wheeler electrons and photons for CP and LP. Much more photons are produced in the LP case than in the CP case due to dynamic features seen in Figs. 2 and 3. Fig. 4(c) gives the particle distributions with respect to χ_e, χ_{ep} and χ_γ parameters for LP. The number of Breit-Wheeler electrons is orders of magnitude greater than that of seed electrons, while their ratio is almost constant for $\chi_e, \chi_{ep} \gtrsim 1$. According to our 2D simulations, 10 Breit-Wheeler pairs are produced per 1 seed electron in the LP SW, indicating a strong avalanche. In the CP SW, this number is 650 times lower.

Different regimes of the electron bunch interaction with two super-intense colliding laser pulses, revealing a transition between the classical (radiation reaction force) and quantum (QED) description, are determined by the laser wavelength and laser intensity [10, 17]. Considering the χ_γ parameter of photons emitted in this interaction, one can determine whether the pair production is exponentially suppressed or a cascade develops. For both CP and LP, we performed a set of simulations with the same parameters as above, but for the laser wavelength in the range from 0.3 μm to 3.0 μm and the laser intensity varying from 1.37×10^{22} W/cm^2 to 1.11×10^{24} W/cm^2. The maximum achieved χ_e, χ_{ep} and χ_γ parameters in the (I, λ) space are presented in Fig. 5. Different regimes of interaction can be distinguished. While for $\chi_e, \chi_{ep} \ll 1$ the radiation reaction is negligible, it is important for $\chi_e, \chi_{ep} \gtrsim 1$. A cascade pair production starts when $\chi_\gamma > 1$. This threshold is achieved with LP laser pulses for much lower intensity than with CP ones. For a given intensity I, higher values of χ_e parameter are achieved as λ grows. As shown above, the χ_{ep} parameter of Breit-Wheeler pairs is greater than the χ_e parameter of seed electrons for both types of laser polarization. This difference is especially significant for CP laser pulses, as seen from Fig. 5. Nevertheless, more intense CP laser pulses are needed to achieve $\chi_{ep} = 1$ in comparison with LP ones. For a given laser intensity I and wavelength λ, the values of χ_e, χ_{ep} and χ_γ are always higher in the case of LP. This is due to the different types of attractors of the dissipative electron dynamics in the CP and LP SW. The presence of loops in the LP SW eases entering the QED dominated regime.

In previous works concluding that the CP SW is more efficient for cascade pair production than the LP SW, e.g., [14], the electron (positron) dynamics is considered exactly in the plane of the electric field antinode on times
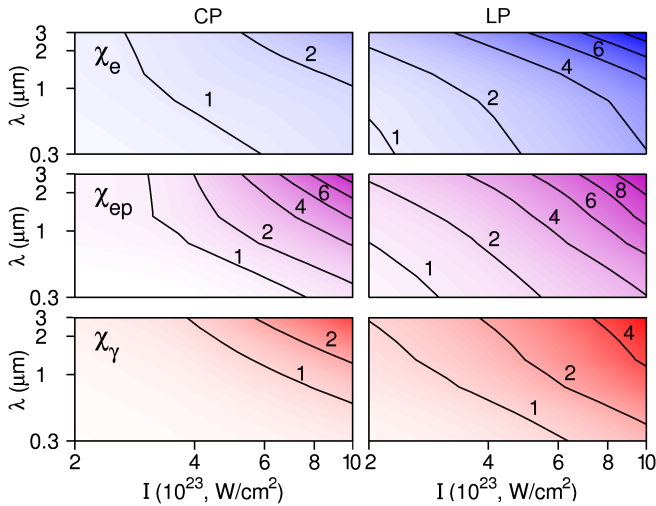
FIG. 5. Maximum χ_e, χ_{ep} and χ_γ parameters vs laser intensity, I, and wavelength, λ, for different laser polarization.
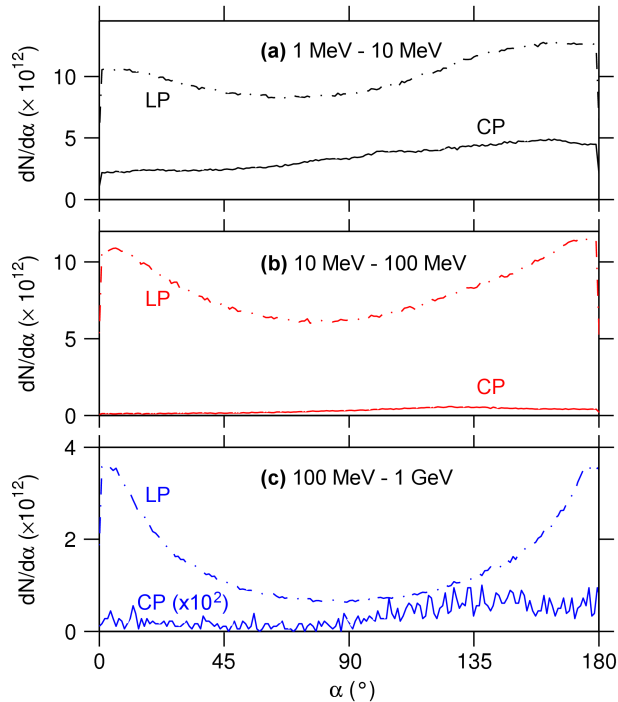

FIG. 6. Angular energy distribution of photons having energy (a) from 1 MeV to 10 MeV, (b) from 10 MeV to 100 MeV and (c) from 100 MeV to 1 GeV. The angle $\alpha = 0^o$ ($\alpha = 90^o$) corresponds to the y-axis (x-axis) direction.

shorter than the trajectory instability development. In contrast, in our case particles have different initial positions, rearranged later by colliding short laser pulses. On the time-scale of few laser cycles particles fall into attractors characteristic to the dissipative system, even if particles initially move exactly in the electric field antinode plane. In addition, the recoil of photon emission at different angles quickly diffuses particles from the electric field antinodes.

The angular distribution of emitted photons also depends on the laser polarization as seen in Fig. 6. In the case of LP, the photons are mainly emitted along the polarization direction being concentrated in the electric field antinode plane. In the case of CP, the photon emission is much lower, especially for higher photon energy.

In conclusion, in the interaction of an electron bunch with two colliding super-intense laser pulses, linearly polarized pulses ease entering the QED dominated interaction regime, facilitating a cascade development and $\gamma e^- e^+$ plasma creation. In contrast to circularly polarized laser pulses, linear polarization provides higher number of Breit-Wheeler pairs having higher energy, which gives much larger emitted photon number. The attractors of the electron motion in the electromagnetic standing wave lead to more efficient photon emission in the linearly polarized standing wave. Oscillating near loops electrons spend more time near electric field antinodes thus producing more Breit-Wheeler pairs and emitting more high-energy photons. Our conclusions are valid for a configuration with obliquely colliding laser pulses considered in a suitable reference frame. We find that with an electron bunch interacting with two colliding linearly polarized laser pulses having the intensity of 5×10^{23} W/cm^2 and wavelength 1 μm, the key parameters satisfy $\chi_e, \chi_\gamma \gtrsim 1$.

[1] ELI Beamlines, www.eli-beams.eu; G. Mourou, G. Korn, W. Sandner, and J. L. Collier, *ELI Whitebook* (Andreas Thoss, Berlin, 2011); G. Cheriaux et al., AIP Conf. Proc. **1462**, 78 (2012); Exawatt Center for Extreme Light Studies (XCELS), www.xcels.iapras.ru.
[2] A. Di Piazza, C. Muller, K. Z. Hatsagortsyan, and C. H. Keitel, Rev. Mod. Phys. **84**, 1177 (2012).
[3] Ya. B. Zel'dovich, Sov. Phys. Usp. **18**, 79 (1975); A. Zhidkov, J. Koga, A. Sasaki, and M. Uesaka, Phys. Rev. Lett. **88**, 185002 (2002); S. V. Bulanov, T. Zh. Esirkepov, J. Koga, and T. Tajima, Plasma Phys. Rep. **30**, 196 (2004).
[4] A. R. Bell and J. G. Kirk, Phys. Rev. Lett. **101**, 200403 (2008).
[5] G. Breit and J. A. Wheeler, Phys. Rev. **46**, 1087 (1934); A. I. Nikishov and V. I. Ritus, Sov. Phys. Usp. **13**, 303

(1970).

[6] V. Ritus, Journal of Soviet Laser Research **6**, 497 (1985).

[7] J. Schwinger, Phys. Rev. **82**, 664 (1951).

[8] S. V. Bulanov, T. Zh. Esirkepov, Y. Hayashi, M. Kando, H. Kiriyama, J. K. Koga, K. Kondo, H. Kotaki, A. S. Pirozhkov, S. S. Bulanov, A. G. Zhidkov, P. Chen, D. Neely, Y. Kato, N. B. Narozhny, and G. Korn, Nuclear Instr. Meth. Phys. Res. A **660**, 31 (2011).

[9] A. Di Piazza, K. Z. Hatsagortsyan, and C. H. Keitel, Phys. Rev. Lett. **105**, 220403 (2010).

[10] S. V. Bulanov, T. Zh. Esirkepov, M. Kando, J. Koga, K. Kondo, and G. Korn, Plasma Phys. Rep. **41**, 1 (2015).

[11] A. M. Fedotov, N. B. Narozhny, G. Mourou, and G. Korn, Phys. Rev. Lett. **105**, 080402 (2010).

[12] S. S. Bulanov, T. Zh. Esirkepov, A. G. R. Thomas, J. K. Koga, and S. V. Bulanov, Phys. Rev. Lett. **105**, 220407 (2010).

[13] N. V. Elkina, A. M. Fedotov, I. Yu. Kostyukov, M. V. Legkov, N. B. Narozhny, E. N. Nerush, and H. Ruhl,

[14] E. N. Nerush, V. F. Bashmakov, and I. Y. Kostyukov, Phys. Plasmas **18**, 083107 (2011); V. F. Bashmakov, E. N. Nerush, I. Y. Kostyukov, A. M. Fedotov, and N. B. Narozhny, Phys. Plasmas **21**, 013105 (2014); E. G. Gelfer, A. A. Mironov, A. M. Fedotov, V. F. Bashmakov, E. N. Nerush, I. Yu. Kostyukov, and N. B. Narozhny, Phys. Rev. A **92**, 022113 (2015).

[15] C. P. Ridgers, J. G. Kirk, R. Duclous, T.G. Blackburn, C. S. Brady, K. Bennett, T. D. Arber, and A. R. Bell, J. Comput. Phys. **260**, 273 (2014).

[16] A. Gonoskov, A. Bashinov, I. Gonoskov, C. Harvey, A. Ilderton, A. Kim, M. Marklund, G. Mourou, and A. Sergeev, Phys. Rev. Lett. **113**, 014801 (2014).

[17] T. Zh. Esirkepov, S. S. Bulanov, J. K. Koga, M. Kando, K. Kondo, N. N. Rosanov, G. Korn, and S. V. Bulanov, Phys. Lett. A **379**, 2044 (2015).

[18] S. S. Bulanov, C. B. Schroeder, E. Esarey, and W. P. Leemans, Phys. Rev. A **87**, 062110 (2013).

Phys. Rev. ST Accel. Beams **14**, 054401 (2011).